PHILOSOPHICAL TRANSACTIONS OF THE ROYAL SOCIETY A
MATHEMATICAL, PHYSICAL & ENGINEERING SCIENCES

The Properties of Drilling Muds at High Pressures and High Temperatures

B. J. Briscoe, P. F. Luckham and S. R. Ren

Phil. Trans. R. Soc. Lond. A 1994 **348**, 179-207
doi: 10.1098/rsta.1994.0088

The properties of drilling muds at high pressures and high temperatures

By B. J. Briscoe, P. F. Luckham and S. R. Ren

Particle Technology, Department of Chemical Engineering, Imperial College of Science, Technology and Medicine, London SW7 2BY, U.K.

This paper describes an experimental study of the rheological properties of various aqueous bentonite suspensions which resemble those oil-well drilling fluids, or muds, which are encountered in practice. Data are presented for systems which are termed 'concentrated' muds, 'thinned' muds and 'barite-loaded' muds, under the conditions which commonly occur during oil-well drilling operations, namely, at high pressures and high temperatures. Concentrated muds comprise of suspensions containing 7–10% (by mass) clay particles. The thinned variety contains similar quantities of clay particles but relatively large amounts of electrolytes. The inclusion of barite particles in these suspensions is a routine commercial means of increasing the density of the media. The data have been obtained by the use of a rolling-ball type rheometer, for performing rheological measurements at pressures up to 1400 bar (1 bar $\approx 10^5$ Pa) and at temperatures up to 140 °C. The rheological response of these model drilling fluids is shown to approximate to those of Bingham fluids. The experimental data, which are reported in terms of two Bingham parameters (a yield stress and a plastic viscosity), show that the application of high pressure modifies the Bingham characteristic parameters in a way which is both temperature and mud composition dependent. The rheology of these muds is found to be shear-history dependent and the extent of this effect is described in terms of a 'ten minute gel strength'. This parameter provides a means of quantifying the thixotropic properties, or gel restructuring rate, of the muds. An induced volume change model, an application of the law of Corresponding States, has been introduced to describe the variations of the Bingham parameters (the yield stress and the plastic viscosity) of the concentrated muds as a function of pressure, temperature and clay content. The model is generally effective for the rationalization of the variation of the plastic viscosity. The model, however, presumes an equilibrium state for the system, and the rationalization of the yield stress data on this basis, particularly at low temperatures, is much less satisfactory. The data suggest that the characteristic gel restructuring times are long compared with the timescale of experiments and hence, complete gel formation may not have occurred during the timescale of our experiments, particularly at lower temperatures. Hence the full plastic yield strength potential was not achieved. At higher temperatures, it appears that the gel structure is more fully recovered within the experimental timescale and the inference is therefore that the gelation process is thermally activated. The data also suggested that thermally induced electrolyte dissolution may be responsible for certain features noted in the temperature dependence of the rheology. In addition, the densities and the sonic velocities of these muds at high pressures and high temperatures are described and discussed.

Phil. Trans. R. Soc. Lond. A (1994) **348**, 179–207

Printed in Great Britain

Vol. 348. A (15 August 1994)

Notation

A_T	temperature-dependent coefficient for yield stress
C_{f}	isothermal coefficient of compressibility
C_{fm}	isothermal coefficient of compressibility of muds
D, d	diameters of tube and ball respectively
P	pressure
S_{y}	exponent of yield stress against clay content relation
T	temperature
T_{D}	critical gel disruption temperature of a mud
T_{R}	critical gel restructuring temperature of a mud
V_1	volume of sample at high pressure high temperature (HPHT) ambient conditions
V_0	volume of sample at room ambient conditions
V_{s}	sonic velocity in fluid
V_{t}	terminal rolling velocity of a ball
α_{p}	pressure coefficient for sonic velocity
$\alpha(\phi)$, $\beta(P)$	factors of packing and compressibility
$\dot{\gamma}_{\mathrm{e}}$	equivalent shear rate imposed by a rolling ball
$\eta_{\mathrm{pl}}(P, T)$	plastic viscosity measured at pressure, P, and temperature, T
$\eta_{\mathrm{pl},1}$	plastic viscosity measured at room ambient condition
$[\eta_{\mathrm{pl}}]$	normalized plastic viscosity
θ	inclined angle of rolling ball rheometer
ρ	density of fluid
ρ_O	density of fluid at room ambient condition or at reference conditions
η_O	viscosity at reference temperature
η_{HB}	high shear viscosity defined by Alderman *et al.*
$\rho_{P,T}$	density of fluid at pressure P, temperature T
ρ_{s}	density of rolling ball
Φ_{w}	clay content by mass or clay mass fraction
ϕ	volume fraction of solid particles
$\Delta\Phi_{\mathrm{w}}$	increase in the effective mass fraction of the bentonite clay brought about by application of an isothermal pressure, compared with ambient
$\bar{\lambda}$	equivalent shear stress parameter for HPHT rolling ball
τ_{B}	the Bingham yield stress
τ_{y}	extrapolated Bingham yield stress
$\tau_{\mathrm{y}}(P, T)$	(extrapolated) yield stress measured at pressure, P, and temperature, T
$\tau_{\mathrm{y},1}$	(extrapolated) yield stress measured at room ambient condition
$[\tau_{\mathrm{y}}]$	normalized (extrapolated) yield stress

1. Introduction

Drilling fluids, such as clay suspensions (muds), usually develop non-newtonian flow characteristics. A number of models, or relations, are available to describe the rheological response, but an accurate and efficient model which describes these flows is that of the Bingham fluid (Bingham 1922). Thus, the Bingham yield stress, τ_{B}, and the plastic viscosity, η_{pl}, may be used to describe adequately, in the limits of low and high shear strain rates at least, their observed rheological properties (Briscoe *et al.* 1992*a*);

$$\tau = \tau_{\mathrm{B}} + \eta_{\mathrm{pl}}\,\dot{\gamma}, \tag{1}$$

where τ is the imposed shear stress and $\dot{\gamma}$ the apparent rate of shear.

Because drilling muds are used under high pressure and high temperature conditions 'downhole' (say pressures up to 1400 bar and temperatures up to 200 °C), a consideration of the pressure and temperature effects on drilling fluid rheology is required for safe and optimal operations (Gray & Darley 1980). Smalley *et al.* (1989) studied the structural properties of n-butylammonium vermiculite at high hydrostatic pressures over a narrow temperature range and, using neutron diffraction, observed a disorder: order phase transition which would have considerable rheological consequences. However, most drilling muds remain in the disordered state under operating conditions. The elevation of the ambient temperature and pressure may influence the rheological properties of a suspension as a result of two additional factors: the variations of the viscosity of the continuous phase and the changes induced in particle–particle (or particle–wall) interactions. The direct effect of the induced temperature and pressure changes on the viscosity of the continuous liquid phase is a first-order factor. However, this influence may be overshadoweed by a stronger influence of the changes in the particle–particle interactions for a highly structured fluid. That is, various electrochemical interactions between the solid particles may be modified. In addition, temperature variation has a significant effect on the activity of the dissolved ions in the aqueous phase and certainly on the solubility of electrolytes. As a result, the consequent changes in the ionic equilibria will alter the force balance between the inter-particle attractive and repulsive forces and hence the flow behaviour of the suspensions. Furthermore, the mean inter-particle separation distance will be reduced during the compression of the liquid phase, with the consequence of an increase of the effective solid volume fraction. These effects will increase the extent of both the elastic and viscous response of the system. An increase of temperature which causes the liquid phase to expand produces the converse effect. Finally, chemical reactions between the phases may be promoted at high temperatures and pressures. These types of process will produce major changes in rheological behaviour of suspensions.

Both the magnitude and direction of these effects will vary with the particular characteristics of a given suspension. There are actually few published experimental studies which quantify these effects for the rheology of aqueous clay suspensions. Annis (1967) studied the rheology of aqueous muds at temperatures up to 150 °C. Hiller (1963) has also studied the effects of applied pressures up to 8000 psi (500 bar). The published results were quite scattered and are not fully interpretable. Annis' experiments with bentonite suspensions at elevated temperatures suggested that high temperatures caused flocculation of the bentonite muds, resulting in an increase of both the yield stress and viscosity at low shear rates. Sinha (1970) investigated water-based clay suspensions as well as oil-based muds using a falling-bob consistometer and suggested that, compared with oil-based muds and inverted emulsion muds, the equivalent viscosity of water-based muds is not affected to the same extent by the variations of temperature and pressure. The equivalent viscosity obtained in his falling-bob rheometer is defined from calibrations with a conventional rheometer; naturally the parameter is a function of the strain rate. However, the effect of pressure on the equivalent viscosity of water-based muds seems to depend on the composition and temperature of the system. He concluded that temperature is the dominating variable in the case of water-based muds. For more complex drilling fluids (e.g. bentonite deflocculated by chrome lignosulphonate), the yield stress ($\tau; \dot{\gamma} \rightarrow 0$) measured by Alderman *et al.* (1988), or the equivalent viscosity at low shear rate reported by Sinha (1970), were weakly dependent on temperatures below a critical temperature, T_{R}, and were essentially independent of pressure. Above T_{R}, the yield stress increases rapidly with increasing temperature; T_{R} is termed here as the 'critical gel restructuring temperature'. The addition of deflocculants decreases the gel restructuring temperature of a mud. The application of high pressures seemed to have practically no effect on the plastic viscosity of a deflocculated mud at low temperatures. However, at higher temperatures (above T_{R}) the effect of pressure becomes significant. Annis (1967) also reported that the time-dependent gel strength (yield value) was the mud property mostly affected by elevated temperatures. Alderman *et al.* (1988) attributed the pressure effect to an effective density change and the compaction of particles during pressurization. There is another critical temperature, reported by Sinha (1970) in his experiments but not interpreted, where the equivalent viscosity of the muds becomes a maximum and then decreases with the further increase of the temperature. This critical temperature, which is much higher than T_{R} (for pure clay mud it is *ca.* 170 °C), is described as the 'critical gel disruption temperature' (T_{D}). Sinha (1970) also suggested that the application of high pressures appeared to aid the formation of gel structures at relatively high temperatures and hence would increase the value of T_{D}.

A simple quantitative and physically based relation has been developed to predict the effects of temperature and pressure on the rheology of deflocculated muds (Alderman *et al.* 1988). In essence, the influences of pressure and temperature are described by separately considering the induced volumetric change in the fluid phase and hence the resulting effects on the inter-particle separation. The changes induced in the rheology of the continuous phase are also introduced. A high shear-rate viscosity, η_{HB}, was derived, on this basis, as a function of temperature and pressure:

$$\eta_{\mathrm{HB}} = \eta_O[1+\alpha(\phi)\,\beta(P)\,P]\exp\left[(E_{\mathrm{u}}+P(BT-C))/kT\right], \tag{2}$$

where η_O is a pre-exponential factor, given by $\eta(T_{\mathrm{r}})\exp(E_{\mathrm{u}}/kT_{\mathrm{r}})$; E_{u} relates to an 'activation energy', T_{r} is the chosen reference temperature and k is the Boltzmann constant. B and C are constants which are characteristics of the continuous phase. The parameter $\alpha(\phi)$, where ϕ is the volume fraction of the particles, represents the particle interaction term whose magnitude is influenced by the ambient pressure via a compressibility term $\beta(P)$. The form of the relation is consistent with the proposition that the effects of the ambient may separately alter the particle–particle interactions as well as the continuous phase rheology. The former is included in part of the pre-exponential term and the latter in the Barus–Eyring type exponential term and the pre-exponential factor (Reid *et al.* 1977). The significance of relations of this sort and their general application are discussed further in the conclusion of this paper.

Empirically, in Alderman *et al.* (1988), the isobaric extrapolated yield stress, τ_{y}, was represented by the following expressions:

$$\tau_{\mathrm{y}} = A_{\mathrm{L}}\exp(-E_{\mathrm{L}}/T), \quad \text{for} \quad T < T_{\mathrm{R}} \tag{3a}$$

and

$$\tau_{\mathrm{y}} = A_{\mathrm{H}}\exp(-E_{\mathrm{H}}/T), \quad \text{for} \quad T > T_{\mathrm{R}}, \tag{3b}$$

where $E_{\mathrm{H}} \gg E_{\mathrm{L}} = 0$. The magnitudes of the parameters $A_{\mathrm{H,L}}$, $E_{\mathrm{H,L}}$ and T_{R} were determined by the measurements of the rheological characteristics at a series of temperatures. The physical significance of these expressions is discussed later. However, the important point is that the yield stress is apparently not a function of temperature below the critical gel restructuring temperature. Above T_{R}, the yield

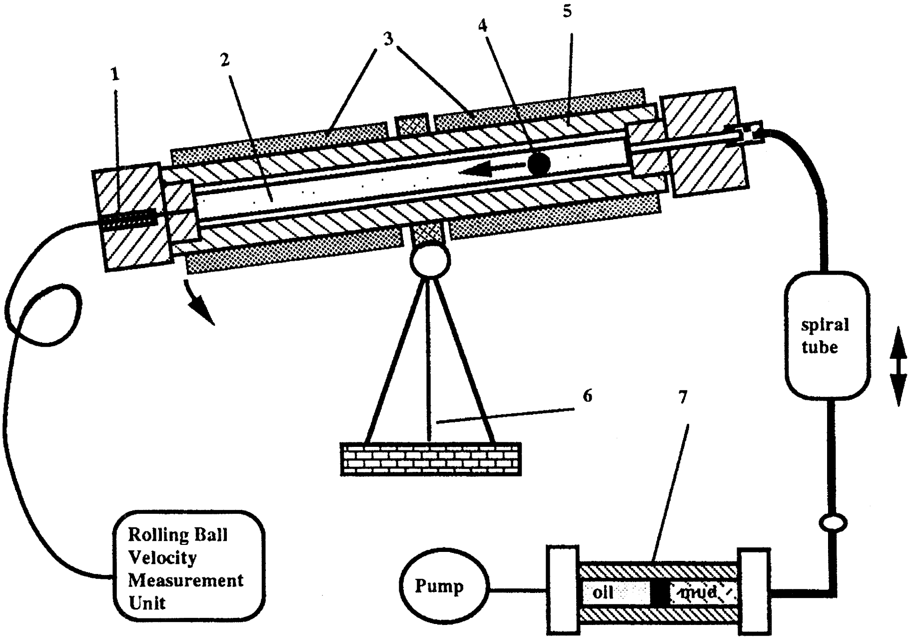

Figure 1. Schematic diagram of the high pressure and high temperature rolling-ball rheometer. 1 wireguide; 2 non-conductive tube; 3 temperature control unit; 4 rolling ball; 5 pressure vessel body; 6 rig frame; 7 oil–mud isolator.

stress increases with an increase in the temperature. These relationships are only reliable for those muds that are fully dispersed and deflocculated. Unfortunately, these previous studies do not fully consider the properties of concentrated muds, such as freshwater clay suspensions with high clay contents. Here, the yield stress is the major parameter and this is sensitive to many other environmental factors.

This paper is mainly concerned with these concentrated bentonite muds. An extended induced effective volume model is derived to interpret the experimental data. The high pressure and high temperature rheological measurements were conducted using a novel high pressure and high-temperature rolling-ball rheometer. The behaviour of thinned muds and barite-loaded muds is also reported. In addition, the ten minute gel strength of some of these muds at high pressures and temperatures are presented. The origins of the pressure and temperature effects on the yield stress and the plastic viscosity of the muds are discussed. Data on other properties of the muds, such as the density and the sonic velocity as a function of pressure and temperature, are also provided.

2. Experimental

(a) *High pressure and high temperature* (HPHT) *rolling-ball rheometer*

(i) *Description of the equipment*

The HPHT rolling-ball rheometer, shown schematically in figure 1, consists mainly of three parts: the high pressure cell, the pressure and temperature control system and the rolling ball velocity measuring system. The heart of the rheometer is the high pressure vessel, which is 76 cm in length and 10 cm in diameter (35 mm internal diameter), constructed from a ductile, hydrogen-embrittlement resistant, stainless

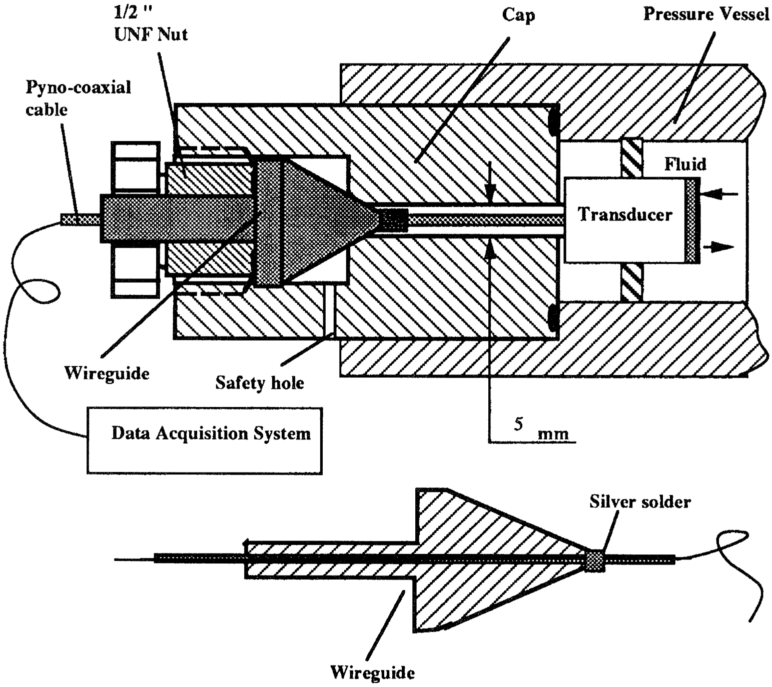

Figure 2. Schematic diagram of the pressure vessel cap and the wireguide

steel. Each end of the vessel was capped with screwed end plugs and sealed with ductile copper gaskets. Both end caps of the vessel contained a standard coned-and-threaded connection. One was used as a high pressure pipe inlet which was connected to a spiral tube unit constructed from high pressure tubing. The other was used to house a signal wireguide (see figure 2). The use of a spiral tube unit (a 6 m length of 6.35 mm high pressure tube formed into a spiral) allows the pressure vessel to rotate through an angle of more than 180°. The pressure vessel was held by a wooden (beech) clamp and attached to a steel shaft housed in an oil impregnated wooden (also beech) bearing.

A metal ball and the fluid sample being studied were enclosed inside the pressure cell. The diameter ratio of the ball to that of the tube used in this study ranged from 0.65 to 0.74. In the measurement, the ball was first located at one end of the vessel while the vessel itself was turned to the horizontal position. When the pressure and the temperature reached the required values, the vessel was rotated to a predetermined inclined angle to allow the ball to roll down along the wall of the tube. Meanwhile, the measuring system was triggered and the movement of the ball was sensed and recorded. Measurements were usually performed with inclined angles, θ, ranging from 1° to 80°, using a frame with 50 stops corresponding to 50 accurately pre-fixed angles (0.01°).

The location of the rolling of the ball could be monitored either by an ultrasonic technique or with an electrical-inductance system. A contact-type piezoelectric ultrasonic transducer (1 MHz, Rolls Royce Mateval, U.K.) has proved very effective and accurate at pressures up to 900 bar and temperatures up to 80 °C. For more extreme conditions, an electrical-inductance system that included an addition of an internal coaxial non-conductive tube was used. The system provided less precision but was more robust. A series of inductive coils (six coils were used in the current study) were wound on the non-conductive (Perspex, glass or ceramic) tube at fixed distances. These coils were connected to form an inductance bridge. The extra non-conductive tube with the coils was enclosed inside the pressure vessel. When an electrically conductive ball rolls inside the tube and passes through each coil, the equilibrium of the inductance bridge is broken in a time base which is used to calculate the rolling velocity of the ball. The working temperature of the system was mainly determined by the endurance of the non-conductive tube and the coils; for example, a Perspex tube would withstand temperatures up to 140 °C, whereas glass and ceramic tubes were used for temperatures above 140 °C.

The hydraulic pressure was produced by an air-driven pump (Airhydro Unit, Charles & Maden Ltd, U.K.) through an intermediate hydraulic oil system. Thus an isolator (piston type) was included to separate the oil and the sample to be studied (as shown in figure 1). The isolation system was constructed with a large volume to facilitate filling and to compensate for leakage and volume expansion. The pumping unit was an air booster unit (ratio 1:250) which was capable of maintaining isobaric conditions (±10 bar) that were predetermined by the pressure of the air supply. The heating of the pressure vessel was achieved by the use of two heating tapes (400 W) wrapped around the pressure vessel. The vessel was thermally insulated. The temperature was monitored and controlled by two thermocouples located on the surface of the pressure vessel. The time lag and thermal gradient between the vessel and interior were established by supplementing experiments. The estimated error in temperature was less than ±5 °C.

(ii) *Principle of the rheometer*

The principle of the application of the rolling-ball geometry for conducting rheological measurements for non-newtonian fluids has been described in previous studies (Briscoe *et al*. 1992*b*). In the use of the rheometer for a comparative study of the pressure and temperature effects on mud rheology, an equivalent normalized shear stress parameter, $\bar{\lambda}$, is defined by considering the stress imposed by the ball and the density variations of fluids at high pressures and temperatures;

$$\bar{\lambda} = \sin\theta\,(\rho_s - \rho_{P,T})/(\rho_s - \rho_O), \tag{4}$$

where $\rho_{P,T}$ is the fluid density at pressure, P, and temperature, T, ρ_O is the fluid density at room ambient and ρ_s the density of the ball. θ is the inclined angle of the tube. An equivalent shear rate, $\dot{\gamma}_e$, imposed by the rolling of a ball with a terminal velocity of V_t, is defined as

$$\dot{\gamma}_e = 4dV_t/(D^2 - d^2), \tag{5}$$

where D and d are diameters of the tube and the ball respectively. In a previous publication, (Briscoe *et al*. 1992*b*) we investigated the effect of the ball size in relation to the tube diameters. In the experiments reported here the gap between the ball and the tube is sufficient for wall effects to be negligible. To intepret the effects of high pressure and high temperatures, a normalized Bingham yield stress, $[\tau_y]$, and a normalized Bingham plastic viscosity, $[\eta_{pl}]$, referred to the room ambient condition, are defined as

$$[\tau_y] = \tau_y(P, T)/\tau_{y,1} \tag{6}$$

and

$$[\eta_{pl}] = \eta_{pl}(P, T)/\eta_{pl,1} \tag{7}$$

where $\tau_y(P, T)$ and $\eta_{pl}(P, T)$ are the yield stress and the plastic viscosity measured at the corresponding pressure, P, and temperature, T, respectively, and $\tau_{y,1}$ and $\eta_{pl,1}$ are the parameters related to the room ambient condition; that is 20 °C and atmospheric pressure. Usually, the Bingham yield stress is the extrapolated value of the stress to zero rate of shear from high shear rates in the stress–shear rate co-ordinates, and the Bingham plastic viscosity is the slope of the stress–shear rate curves at high shear rates. By defining the normalized parameters $[\tau_y]$ and $[\eta_{pl}]$, the relative values of $\tau_y(P,T)$ and $\eta_{pl}(P,T)$ may be directly obtained from the rheogram of the rolling-ball rheometer; $\bar{\lambda}$ against $\dot{\gamma}_e$ (see Appendix). Thus the experimental data from the HPHT rolling-ball rheometer are interpreted without the need for further calibrations using a 'standard' or conventional rheometer, although good absolute agreement (in terms of τ_y and η_{pl}) between a Bohlin VOR rheometer (Bohlin Reologi, Sweden) used in a standard Couette configuration and the rolling-ball system has previously been obtained (Briscoe *et al.* 1992*b*).

(iii) *Operation of the rheometer*

About 600 ml of sample were needed to charge the pressure cell. The formation of air bubbles was reduced by adopting a gentle filling procedure. Under normal operating conditions, a heating ramp was applied to reach the required temperature. A thermal equilibration time of three hours was used after subsidiary investigations of the heat transfer characteristics of the system. Then pressure was applied at different levels under isothermal conditions. Measurements at several tube inclination angles were carried out to provide sufficient data for plotting the $\bar{\lambda}-\dot{\gamma}_e$ curve. The pressure was then removed. A new temperature level was then selected. For water-based samples, an initial pressure (of 100 bar) was applied to prevent water vaporization when the temperature was above 100 °C.

In measuring thixotropic suspensions, it is crucial to reproduce the same shear-history for each measurement. In the rolling-ball rheometer, the shear-history may be controlled to some extent by allowing the sample to stand quiescent for a fixed time period after applying a chosen amount of shear work. The pre-shearing of the sample was achieved by 'rocking' the tube to allow the ball to roll 'down' and 'up' for a fixed number of times; a fixed rolling angle was chosen for this pre-conditioning. Clearly, this pre-shearing process does not provide a highly defined amount of pre-shear. It does, however, allow an 'equilibrium' amount of shear to be introduced where the rolling ball velocity attains consistent terminal values during successive 'rolls'. This enables two different types of measurements to be undertaken conveniently: an initial yield stress (or plastic viscosity) measurement and a time-dependent gel strength measurement, e.g. a 'ten minute gel strength' such as has been defined in the drilling mud industry for the Fann-type viscometers and Shearometers (Gray & Darley 1980). The time-dependent gel strength is an indication of the degree of the potential thixotropy of the muds. The data are useful to determine the cuttings-suspending-capacity of drilling fluids after the mud circulation is stopped, and also to calculate the pump pressure required to re-establish the circulation after the mud has remained quiescent for a period of time inside the well. In this study, data were collected, both when the mud had received no pre-shearing and when the mud was pre-sheared, followed by a pause of ten minutes before further experiments were performed. In this way a measure of the time-dependent gel strength of the system could be obtained.

(*b*) *Experimental errors*

The errors which appear in the estimation of the yield stress and the plastic viscosity of clay suspensions using the HPHT rolling-ball rheometer may associate with three terms: (i) the intrinsic errors associated with the use of the rolling-ball rheometer; (ii) the errors introduced in the extrapolation using limited experimental data; (iii) the errors associated with the adoption of the flow model chosen which may not be valid for all the conditions considered (e.g. under high pressures and temperatures). The first term has been estimated by parallel measurements with the same materials using both the rolling-ball system and a conventional rheometer (a Bohlin VOR rheometer). The results have been published elsewhere (Briscoe *et al.* 1992*b*). Generally speaking, the errors or certainties associated with the rolling-ball method, compared with the Bohlin rheometer, are under 8% for the yield stress measurements in the range 1.8–27 Pa. For the plastic viscosity, this error is under 10%. The curve fitting errors, with the limited experimental data, (usually 6–12 data points were used; see figures 4 and 5) have been estimated as under 5%. The error introduced by using the Bingham approximation as a generic fitting expression is of a different sort, although naturally it is influenced by the choice of the number of data points and their distribution within the shear rate axis. Actually, the important data points are those taken at relatively high strain rates where errors are smaller. The important point, however, is that the two parameters, the yield stress and the plastic viscosity obtained are defined within the context of the Bingham model. The model and these parameters will provide a reasonable reproduction of all the experimental data. More importantly, however, the two parameters provide an economic and accurate (within the limitations described) description of two of the fluid's critical rheological response characteristics; its inherent plasticity and viscosity.

(*c*) *Compressibility and density measurements*

A modified mercury porosimeter (Series 800, Carlo Erba Instrumentazione, Italy) was used to determine the compressibility of the mud samples at room temperature. The fluid sample was contained in a rubber bag which was enclosed in the autoclave. The volume decrement of the sample as a function of pressure was measured and the density computed. The isothermal coefficient of compressibility of materials (Perry & Green 1985), C_f, is calculated as

$$C_f = -\frac{1}{V_O}\frac{d(V_O - V)}{dP}, \tag{8}$$

where V_O is the volume of the sample at room ambient, and V the volume of the sample at pressure, P. In the measurement, appropriate correlations were also made to account for the compressibility of the mercury and the rubber membrane. C_f was not found to be a function of pressure up to 1200 bar.

(*d*) *Sonic velocity measurements*

Data for the sonic velocities of the muds are required in the use of the ultrasonic technique adopted to monitor the descent of the rolling ball in the rheometer described. The measurements of the sonic velocity as a function of pressure and temperature were conducted using a device which was fixed into the high-pressure cell and is shown schematically in figure 3. The sound wave produced from the

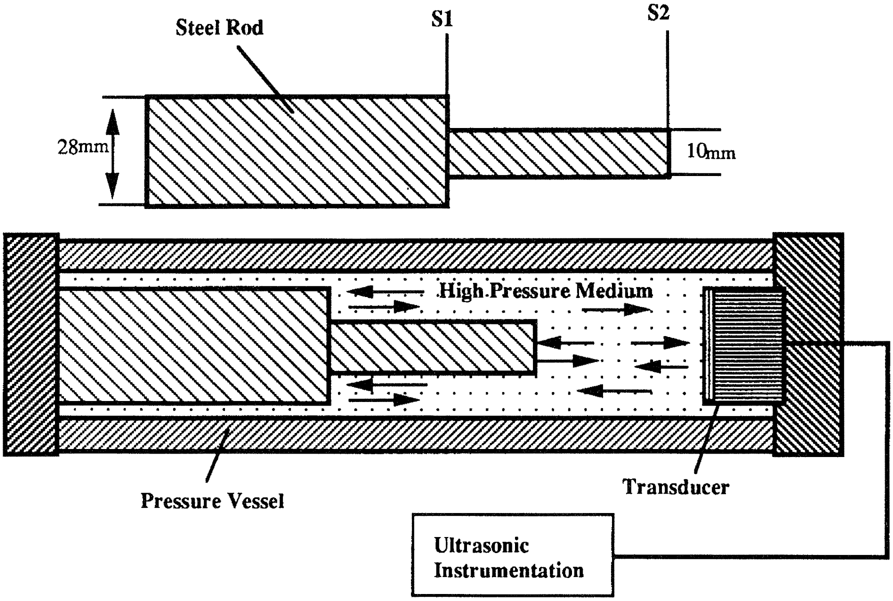

Figure 3. Schematic diagram of the device for measuring sonic velocity in fluid materials at high pressures.

transducer is reflected from the two surfaces (S1 and S2 sections in figure 3) which are separated a certain distance on the rod. The measured time delay allows the sonic velocity to be computed. Studies of the sonic velocities of water or seawater as a function of pressure, temperature and salinity, have been well documented (Wilson 1959, 1960, 1962). A significant observation from the previous studies is that the effects of all these factors on the sonic velocity are additive. This means that the description of the sonic velocity, as a function of these variables, can be obtained in an economic way.

(*e*) *Materials*

A sodium-based bentonite powder (ASB 350 S), supplied by the ECC International (U.K.), was used in this study without any further purification. The clay suspensions were prepared by mixing a known weight of the bentonite powder with doubly distilled water using a Silverson high shear mixer for ten minutes. The initial pH of the clay suspension was measured as 10.0 ± 0.5. The barite powder (barium sulphate) used in the experiments was a commercial material obtained from B. W. Mud Ltd (Aberdeen, U.K.), and was passed through a 53 μm sieve. The measured barite particle size (after passing the sieve) ranged from under 1 μm up to 30 μm. Barite is a chemically and electrically inert material with high specific gravity (4–4.6; compared with clay of 2–2.3) and has been widely used as a ‘weighting material’ in drilling fluids.

The mud compositions cited throughout the paper are given in terms of a dry powder mass fraction because bentonite is known to swell in water, making any estimation of volume fraction both impractical and imprecise.

Table 1. *Compressibility of water and muds*

material	ρ at 1 bar calculation[a]	$C_f \times 10^{-5}$ (1/bar) measurement	$C_f \times 10^{-5}$ (1/bar) calculation[b]	ρ at 1000 bar[c] (kg m^{-3})
water	1000	-4.1 ± 0.15	—	1043
7% mud	1034	-3.8 ± 0.15	-3.96	1075
10% mud	1048	-3.7 ± 0.15	-3.90	1082

[a] Based on zero volume of mixing (density of clay 2000 kg m^{-3}).

[b] Assuming particles are incompressible.

[c] Calculated based on the value of C_f from the measurement.

3. Results

(*a*) *Density*

The compressibility values of water and mud samples calculated from the experimental data at room temperature are listed in table 1. The current experimental data have been compared with the experimental results reported by Hoberock *et al.* (1982) and the predictions from a modified relationship given by Kutasov (1988); the comparison is tabulated in table 2. Kutasov's original expression is given in Imperial units; in SI units it may be written as

$$\rho_{P,T} = \rho_O \exp(aP + b(T-15) + c(T-15)^2), \tag{9}$$

where P is pressure (bar), T temperature (°C), and ρ_O the density of the muds (kg m^{-3}) at $P = 1$ bar, $T = 15$ °C. a, b and c are constants dependent on the composition of the suspension. Here, we have re-formulated these constants to a first order approximation, referred to the previous experimental results of McMordie *et al.* (1982), as

$$\left.\begin{aligned} a &= 5.70 \times 10^{-5} - 7.13 \times 10^{-7}\rho_O, \\ b &= -(6.68 \times 10^{-4} - 0.23 \times 10^{-6}\rho_O), \\ c &= -1.47 \times 10^{-6}. \end{aligned}\right\} \tag{10}$$

The present experimental results show that equations (9) and (10) provide a reasonable prediction of the density of muds at high pressures and temperatures; see table 2. These results have been used for correcting the densities of the muds when their rheological measurements are carried out under the high pressure and high temperature conditions reached during the current studies.

It is clear that the presence of clay material in water reduces the compressibility of the system. More interesting, however, is the indication that the observed compressibility reasonably scales, within experimental error, with the water content, assuming that the clay particles are incompressible. An assumption to this effect, for modelling purposes, will be adopted later. It is also noteworthy that there is a positive excess volume of mixing which is consistent with the formation of a gel structure.

(*b*) *Sonic velocity*

In this study, the sonic velocities of the muds as well as that of water, as a function of pressure, temperature and clay mass fraction (Φ_w) have been measured. A general equation for the sonic velocity, which is used in the ultrasonic tracking technique for

Table 2. *Densities* (kg m^{-3}) *of water and muds under pressure and temperature; comparison with the literature*

material	P/bar	T/°C	experiments	Hoberock's data	equations (9), (10)
water	1000	20	1043	1036	1045
water	1000	135	—	978	949
water	1380	165	—	966	937
7% (mass) mud	1000	20	1075	—	1119
10% (mass) mud	1000	20	1082	—	1149

monitoring the rolling of the ball, relating the temperature, the clay concentration and the pressure, may be written as

$$V_s = 1479 - 40\Phi_w + \alpha_p P + 2.72(T-20) - 0.024(T-20)^2, \tag{11}$$

where α_p is the pressure coefficient whose value ranges from 0.171 to 0.166 for muds with clay contents up to 10% (by mass). It will be seen that V_s is relatively independent of Φ_w in the range of the clay content studied in this work. The presence of relatively high particle fractions does not significantly affect the velocity of the wave propagation. Similar trends have previously been seen in composite systems (Briscoe & Zakaria 1992).

(c) *Rheology*

The types of bentonite mud studied involved pure bentonite–water suspensions, $CaCl_2$-treated muds and barite-loaded clay suspensions. The concentration of the bentonite clay ranged from 3% to 12% (mass). The rheological data are presented in five sections. The first two sections deal with concentrated muds at ambient and elevated temperatures respectively. The third section describes the ten minute gel strength behaviour. The final two sections report data on dilute and thinned muds and also on the barite-loaded muds. Unless otherwise stated, the measurements were taken 30 s after the establishment of a consistent series of terminal velocities following the repeated rolling of the ball in the tube.

(i) *Concentrated muds at room temperature*; *ca.* 20 °C

These experiments were carried out at room temperature which varied naturally from 16 °C to 27 °C according to season. The temperature effects on the rheological properties of muds were found to be minimal for changes in the range 10 °C to 30 °C. This fact allowed the experiments to be conducted at various room ambients throughout the seasons without the need for the room temperature to be controlled. The rolling-ball measurements were taken at each pressure level from 1 bar up to 1350 bar. The equivalent rheological parameters were calculated, based on equations (4)–(7), for the samples at each applied pressure.

For all the concentrated muds studied, including pure clay suspensions (7%, 8%, 9%, 10% by mass) and a calcium-treated mud (12% clay + 0.5% $CaCl_2$), it was found that the measured yield stress values were, within experimental error, independent of the ambient pressure. The normalized Bingham yield stresses and plastic viscosities for all the samples tested are listed in table 3. It is clear that, as the pressure increased from 1 bar to 1350 bar, the normalized yield stress fluctuated as much as ±5%, excepting perhaps the 10% mud where the yield stress increased gradually as the pressure increased. On the other hand, the normalized plastic

PHILOSOPHICAL TRANSACTIONS OF THE ROYAL SOCIETY A MATHEMATICAL, PHYSICAL & ENGINEERING SCIENCES

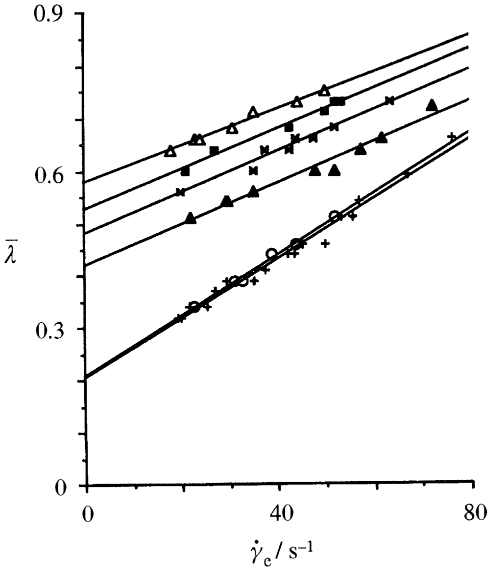

Figure 4. Equivalent shear stress against equivalent shear rate for a 8 % clay mud measured from HPHT rolling-ball rheometer. P/bar, T/°C. △, $P = 1350$, $T = 65$; ■, $P = 1000$, $T = 65$; $*$, $P = 700$, $T = 65$; ▲, $P = 70$, $T = 65$; +, $P = 1$, $T = 22$; ○, $P = 1350$, $T = 22$.

Table 3. (*a*) *Normalized yield stress* $[\tau_y]$ *and* (*b*) *the plastic viscosity* $[\eta_{pl}]$ *of muds under pressures (bar) at room temperature*

	mud (mass %)	T/°C	$P = 1$	$P = 700$	$P = 1000$	$P = 1350$
(*a*)	7	16	1.00	0.96	0.98	—
	8	26	1.00	1.03	0.95	1.00
	9	20	1.00	1.00	—	—
	10	20	1.00	1.03	1.05	1.08
	$12 + 0.5$ Ca^{2+}	21	1.00	0.95	0.95	1.00
(*b*)	7	16	1.00	1.05	1.12	—
	8	26	1.00	1.05	1.07	1.08
	9	20	1.00	1.04	—	—
	10	20	1.00	1.00	1.02	1.13
	$12 + 0.5$ Ca^{2+}	21	1.00	1.04	1.07	1.07

viscosity values (shown in table 3) tended to increase for all the muds studied as the pressure increased, although the magnitudes of the changes were small.

(ii) *Concentrated muds at higher temperatures*; 50–120 °C

The effect of the applied pressure on the rheological properties of the muds was found to be much larger at higher temperatures, however. Figures 4 and 5 present two typical experimental results plotted as the rheograms of the HPHT rolling-ball rheometer; the equivalent shear stress parameter, $\bar{\lambda}$, against the equivalent shear rate, $\dot{\gamma}_e$. Figure 4 presents the data for an 8 % clay mud at various pressures and at a temperature of 65 °C compared with the results obtained at 22 °C. It is clear that, at higher temperatures, the mud is 'thickened' and the apparent yield stress increases with the elevation of the pressure. This is in contrast to the response of the mud at room temperature where the pressure effect (from 1 bar to 1350 bar) is

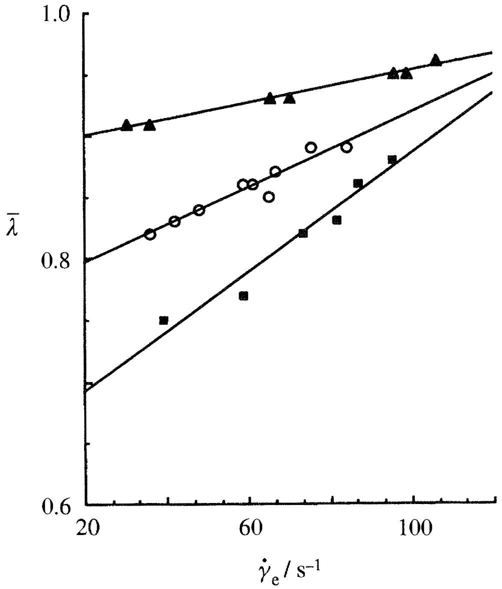

Figure 5. Equivalent shear stress against equivalent shear rate for a 12% clay mud containing 0.5% $CaCl_2$ (mass), measured from HPHT rolling-ball rheometer. P/bar, T/°C. ■, $P = 200$, $T = 115$; ○, $P = 700$, $T = 115$; ▲, $P = 1350$, $T = 115$.

Table 4. (*a*) *Normalized yield stress* $[\tau_y]$ *and* (*b*) *plastic viscosity* $[\eta_{pl}]$ *of muds at high pressures and temperatures*

(Ca^{+2}-mud refers to a 12% clay mud containing 0.5% $CaCl_2$.)

	muds (mass %)	T/°C	$P = 1$	$P = 700$	$P = 1000$	$P = 1350$
(*a*)	7	50	1.54	1.62	1.72	—
	7	70	1.79	1.95	2.04	—
	8	40	1.25	1.50	—	1.65
	8	65	2.1	2.35	2.65	2.90
	8	80	3.05	3.29	3.39	3.60
	10	40	1.38	—	1.62	1.84
	Ca^{+2} mud	70	1.15	1.47	—	1.89
	Ca^{+2} mud	115	1.64	1.97	—	2.28
(*b*)	7	50	0.57	0.67	0.67	—
	7	70	0.67	0.55	0.48	—
	8	40	0.86	0.79	—	0.70
	8	65	0.68	0.68	0.67	0.61
	8	80	0.54	0.54	0.63	0.61
	10	40	0.80	—	0.83	0.60
	Ca^{+2} mud	70	1.29	0.89	—	0.54
	Ca^{+2} mud	115	0.86	0.54	—	0.23

insignificant. The variation of the equivalent plastic viscosity (the slope of the curves) as a function of pressure was insignificant in this case showing that it is not a sensitive parameter with respect to pressure. Similar results for the pressure effects on the same mud sample were also obtained at various temperatures; e.g. 40 °C and 80 °C (results shown in table 4). Unfortunately, with further increases in the temperature (to 100 °C), the 8% mud became too thick to allow the steel ball to roll

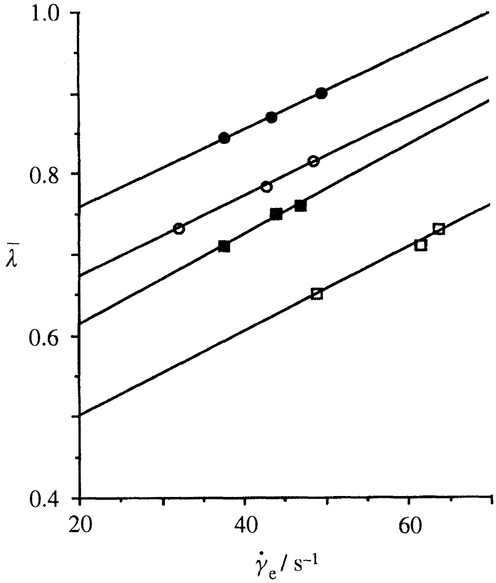

Figure 6. Rolling-ball rheogram showing the time-dependent gel strengths for a 10% clay mud at $T = 24$ °C, $P = 1$ bar. □, Fast-roll; ■, 10 min gel; ○, 20 min gel; ●, 60 min gel.

down the tube, even at the inclined angle of 90°. In the case of the 12% clay mud containing 0.5% calcium chloride (figure 5), measurement was carried out up to 115 °C because calcium ions inhibited the temperature sensitivity of the suspension. Clearly again, the apparent yield stress is enhanced at high pressures and, in addition, the equivalent plastic viscosity now tends to decrease as the pressure increases. This suggests that the system becomes more 'gelled' in character at high pressures and temperatures.

(iii) *The ten minute gel strength*

The thixotropic characteristics of clay suspensions may be demonstrated by carrying out a time-dependent gel strength measurement in the rolling-ball rheometer. Figure 6 presents a typical rheogram of this kind of measurement for a 10% (mass) pure bentonite mud at room ambient conditions. It suggests that, as the standing time (after a fixed pre-shearing history) of the sample increases, the measured gel strength (i.e. the intercept of the curves in the figure) increases steadily. This indicates that the disrupted gel structure of the clay particles is gradually restored as time lapses after shear. These data naturally pose a question as to how the ambient pressure and temperature influence this time-dependent gel restoration process for these clay muds. These studies have also been conducted for different muds. Figure 7 shows the results for a 12% clay mud containing 0.5% $CaCl_2$. In the rolling-ball rheogram shown in figure 7, two sets of the ten minute gel strength experimental data, at different temperatures, are presented. The data suggest that, at room temperature ($T = 22$ °C), the effect of pressure on the gelation restoration rate of the muds is insignificant. However, at a higher temperature ($T = 100$ °C), the mud seems to be thickened more rapidly at the higher pressures. This coincides with the results of the pressure effect on the yield stress behaviour of the muds; the sensitivity of the pressure effect on the gelation of the muds is apparently temperature dependent. Figure 8 shows another example of the ten minute gel

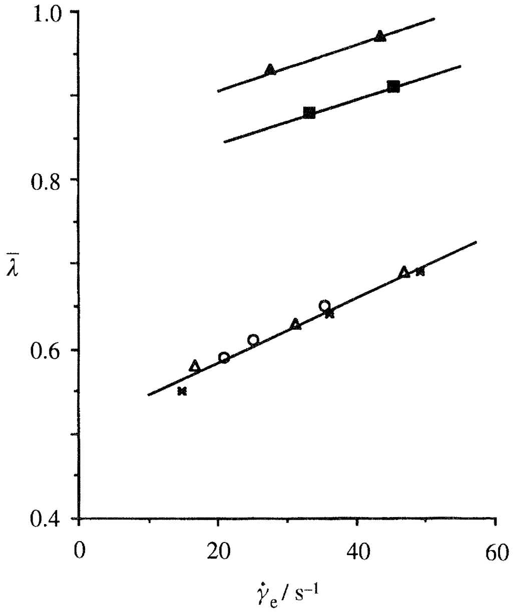

Figure 7. Rolling-ball rheogram showing the 10 min gel strength measured for a 12% clay + 0.5% $CaCl_2$ mud at various temperatures (°C) and pressures (bar). △, $P = 1$, $T = 22$; ○, $P = 900$, $T = 22$; ∗, $P = 1300$, $T = 22$; ■, $P = 170$, $T = 100$; ▲, $P = 700$, $T = 100$.

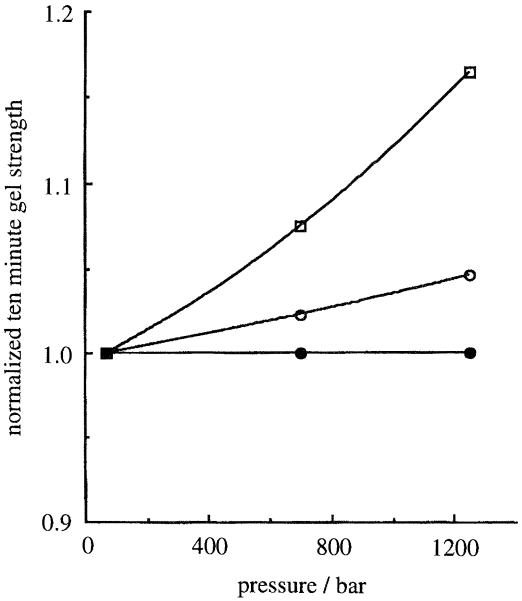

Figure 8. Normalized 10 min gel strength against pressure for a 8% clay mud at various temperatures (°C). ○, $T = 80$; □, $T = 65$; ●, $T = 27$.

strength test for an 8% (mass) pure bentonite suspension. The normalized ten minute gel strength as a function of pressure was calculated by normalization of the data for a pressure of 70 bar. It is apparent again that the ten minute gel strength of the mud is enhanced at high pressures but only at relatively high temperatures;

Table 5. *The rheological properties of the dilute and thinned muds at* HPHT
(Ca^{+2}-mud refers to a 9.6% clay mud containing 1% CaCl$_2$.)

muds (mass %)	T/°C	Bohlin data		HPHT rolling-ball data: τ_y (Pa) only		
		τ_y/Pa	η_{pl}/(mPa s)	$P = 1$	$P = 1000$	$P = 1400$
3	22	0.83 ± 0.5	5 ± 1	0 ± 0.5	0 ± 0.5	0 ± 0.5
3	85	2.5 ± 1	4 ± 1	2.9 ± 1	2.5 ± 1	2.9 ± 1
3	135	—	—	3.4 ± 1	3.1 ± 1	3.1 ± 1
Ca^{2+}-mud	24	3.0 ± 1	8 ± 1	2.4 ± 1	2.6 ± 1	4.9 ± 1
Ca^{2+}-mud	70	6.8 ± 1	7 ± 1	5.6 ± 1	5.2 ± 1	5.6 ± 1

say above 65 °C. We may suppose that, even at lower temperatures, the influence of the applied hydraulic stress on the yield behaviour will be detectable but only after a much longer time of exposure.

(iv) *Dilute and thinned muds*

Here 'dilute' mud refers to the clay suspensions of low solid content and 'thinned' mud denotes the muds which were thinned (showing low yield stress) by certain treatments (e.g. simple bentonite suspensions containing electrolytes at relatively high concentrations). In the former case, the clay platelets are quite well separated and hence the magnitudes of the particle interaction energies are relatively small. In the latter case, the interaction between the particles is 'weakened' because the extent of their electrical double layers are 'compressed' by the electrolytes. The temperature sensitivity of the yield behaviour of these muds is reduced and also the systems show relatively low τ_y/η_{pl} ratios. In both cases, the Bingham yield stress values of the suspensions are relatively low. In the experiments, a 3% (mass) pure clay mud and a 9.6% mud containing 1% CaCl$_2$ were studied. The experimental results, from both a Bohlin rheometer at ambient conditions and the HPHT rolling-ball rheometer at high pressures and high temperatures, are presented in table 5. The rolling-ball data presented here have been calibrated with measurements obtained from a Bohlin VOR rheometer (see Briscoe *et al.* 1992*b* for details of this procedure). The data in table 5 make it clear that the measured yield stress of these dilute and thinned muds is less dependent on pressure compared with the concentrated thicker muds described earlier. The results of ten minute gel strength measurements were found to be similar to the yield stress for these muds; that is the ten minute gel strength is independent of the pressure applied. The calculated plastic viscosities of these muds are also less sensitive to both temperature and pressure.

(v) *Barite-loaded muds*

The effect of temperature on the rheology of the barite-loaded muds at atmospheric pressure has been discussed elsewhere (Briscoe *et al.* 1992*c*). The temperature sensitivity of the yield behaviour of barite-loaded muds is mainly attributed to the activity of the bentonite particles; the barite particles retain their 'inertness' at these higher temperatures. A clay–barite mud, with 6% (mass) clay and 60% (mass) barite content, was further studied using the HPHT rolling-bar rheometer. The experimental results are generalized in figure 9, where the equivalent shear stress

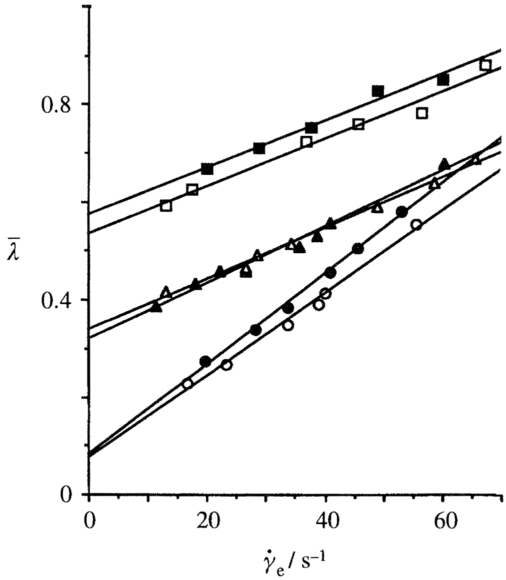

Figure 9. Rolling-ball rheogram for a barite-loaded mud (clay 6%, barite 60%, mass) at various pressures (bar) and temperatures (°C). ○, $T = 27$, $P = 1$; ●, $T = 27$, $P = 1350$; △, $T = 65$, $P = 70$; ▲, $T = 65$, $P = 1350$; □, $T = 85$, $P = 100$; ■, $T = 85$, $P = 1350$.

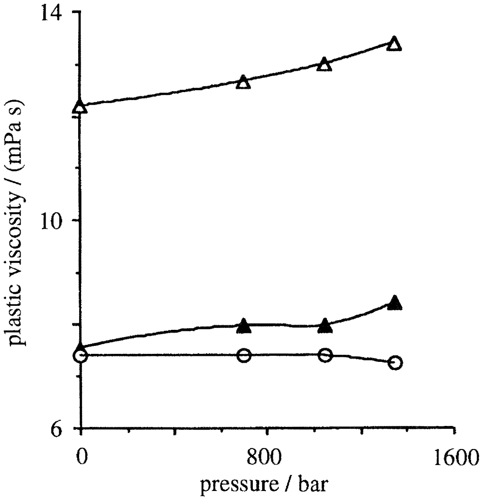

Figure 10. Plastic viscosity versus pressure measured for a barite-loaded mud (clay 6%, barite 60%, mass) with HPHT rolling-ball rheometer at various temperatures (°C). △, $T = 27$; ▲, $T = 65$; ○, $T = 85$.

parameter, $\bar{\lambda}$, against the equivalent shear rate (the HPHT rolling-ball rheogram) is plotted for the mud at various temperatures (27 °C to 85 °C) and high pressures up to 1350 bar. As may be seen from figure 9, the increase of the apparent yield stress (the intercept of the $\bar{\lambda}$–$\dot{\gamma}_e$ curves at zero shear rate) with the increasing temperature is similar to that observed for unweighted muds. The apparent plastic viscosity (the slope of the curves) decreases as temperature increases. The influence of pressure on the plastic viscosity and the yield stress behaviour of the muds are represented

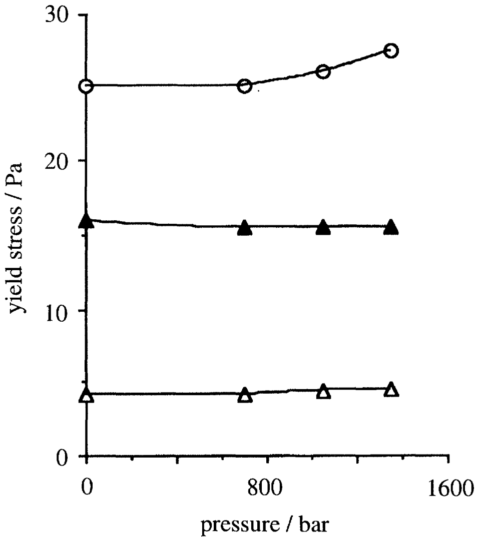

Figure 11. Yield stress versus pressure measured for a barite-loaded mud (clay 6%, barite 60%, mass) with HPHT rolling-ball rheometer at various temperatures (°C). △, $T = 27$; ▲, $T = 65$; ○, $T = 85$.

respectively in figures 10 and 11. At low temperatures (e.g. 27 °C and 65 °C), the plastic viscosity of the mud increases with increasing pressure in a similar way to, but more strongly than, that observed for unloaded muds. However, at higher temperatures, not only are the absolute values of the plastic viscosity reduced as the pressure is increased, but they also become independent of the pressure applied; for unloaded muds no significant effects were found in the plastic viscosity at elevated temperatures as a function of pressure. The observed yield stress behaves differently. At low temperatures, the yield stress is independent of pressure, but increases slightly with increasing pressure at higher temperatures. In summary, the introduction of the barite particles significantly alters the influence of pressure on the rheology of the suspension. The plastic viscosity response to pressure, like that of the original muds, increases with the applied pressure but somewhat more strongly. However, at elevated temperatures this increase is reduced. As for the yield stress parameter, again in comparison with the unloaded mud, the application of pressure has no influence at ambient temperatures. At high temperatures, there is a detectable increase but this is less apparent with the barite loaded systems than with the unloaded muds.

In summary, although the trends seen in the unloaded muds is apparent, the extent of the pressure and temperature induced changes in the yield stress response is reduced. This may be associated with the inevitable increase in electrolyte concentration provided by the addition of barite powders. An electrical conductivity measurement of the abstracted water from a 60% (by mass) barite–water suspension has been carried out and confirms an ionic strength increase of the mud aqueous phase induced by the addition of the barite particle. These results show that the addition of the barite (60% by mass) will provide a 30% increase of the ion concentration of the aqueous phase of the mud. To investigate this effect further, atomic absorption spectroscopy of the abstracted water from the barite–water suspension was undertaken. The results are presented in table 6. They show that the

Table 6. *Atomic absorption spectroscopy analysis of abstracted water from barite suspensions*

samples (mass %)	concentration/(mg d m^{-3})		
	Ba^{2+}	Ca^{2+}	Na^{+}
20 (mass) barite	1.2	17.8	32.3
40 (mass) barite	1.6	22.9	43.6
60 (mass) barite	1.2	25.4	55.6
4 clay aqueous phase	0.7	0.3	631.0

Table 7. *Conductivity of aqueous phases*

samples	conductivity/(μs cm^{-1})	value relative to water
preparation water	60	1
6 % clay (mass)	1080	18
60 % barite (mass)	210	3.5
0.5 % $CaCl_2$ solution	1550	25.8

solution is saturated with barium ions (*ca.* 10^{-5} M) and that calcium and sodium are also present but not in a saturated state (e.g. 60 % barite–water suspension contains *ca.* 5×10^{-4} M of Ca^{2+} and *ca.* 2.5×10^{-3} M of Na^{+}). Thus, it appears that it is the introduction of these liberated cations (Ca^{2+} and Na^{+} are present as impurities in the barite) from the barite powder into these muds, which in part suppresses the overall rheological sensitivity to temperature and pressure of the weighted muds.

The relative contribution from each constituent of the mud to the electrolyte balance was obtained by measuring the conductivity of the various constituents of the muds, namely, (i) preparation water, (ii) abstracted water from mud and (iii) abstracted water from barite suspensions. These data are given in table 7. The effective electrolyte environment is dominated by the electrolytes released from the clay materials. The calcium-treated mud (e.g. 0.5 % $CaCl_2$) contained about 25 units of electrolyte (referred to preparation water; table 7) provided by $CaCl_2$, which is a significantly higher contribution than that provided by the other components. It is apparent that the introduction of $CaCl_2$ to produce the thinned muds provides a major increase in electrostatic screening. The contribution from the barite is much smaller but its effect on the rheology of the muds is apparent (also see Briscoe *et al.* 1992*c*). We have also investigated the effect of temperature on the conductivity of the water-based muds. We observed that heating up to 80 °C increased the conductivity of the system by 50 %. Clearly, more cations (Na^{+} for pure clay muds) are dissolved from the surface of the clay particles at higher temperatures. On cooling, a rapid decrease of the conductivity was noted which indicates that the ionic dissolution process is reversible as one would expect.

4. Discussion and modelling

These data, and the associated analysis, provide only a fragmented description of what is clearly a rather complex combination of the effects which ultimately combine to give a characteristic rheological response. The data have been modelled by approximation as exhibiting linear combination of an intrinsic plastic yielding a newtonian fluid response, and two descriptors have been abstracted: an extrapolated

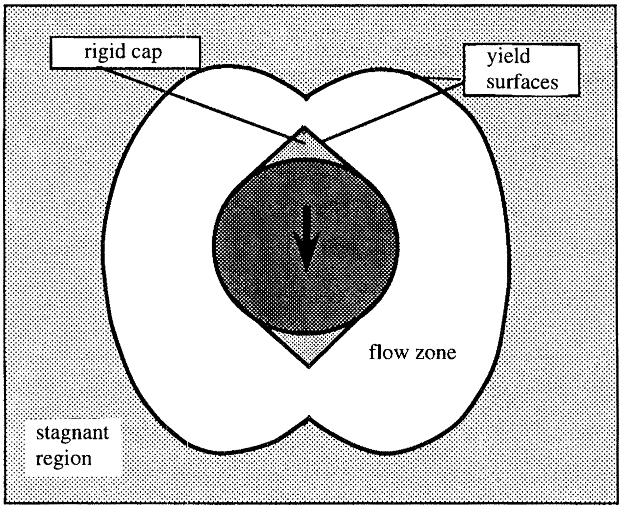

Figure 12. Schematic diagram of a falling sphere in a Bingham fluid (from Beris *et al.* 1985).

Bingham yield stress and a Bingham (plastic) viscosity respectively. We have thus supposed that the rheology of the various fluids may be sufficiently described by a low strain time-dependent characteristic and a higher strain rate time-invariant property. The former describes the stress required to institute flow and the latter the stress required to maintain flow. The nature of the rolling ball rheometer is such that the rolling ball mobilizes a fluid zone around itself as it passes through the essentially stagnant, plastically yielding fluid. The form of this fluid envelope, which will not be distinct around the ball, is not established for the rolling ball case, but, for the falling ball configuration, the shape is most probably a toroid. Figure 12 shows the form we believe to be established for a falling-ball in a Bingham fluid which supposes an instantaneous recovery of the gel structure in the trailing zone (Beris *et al.* 1985). We may speculate that a similar, but distorted, toroid is produced in the rolling ball experiment. The body forces disturb and fluidize the mud ahead of, and behind, the ball as it rolls down the tube. This fluidized layer ultimately recovers its plastic and gel character. Intuitively, we expect that the geometry of the forward front will be defined mainly by the plastic viscosity at the prevailing rate of deformation and the yield stress of the stagnant medium. The position of the trailing interface will be defined similarly. In addition, the location of the trailing zone is also a function of the rate of recovery of the gel structure of the medium.

The data provided indicate that both the viscous and plastic characteristics are functions of the particle concentration (and the electrolyte concentration), the temperature and the hydraulic pressure. What is more, these characteristics, particularly the plastic component, are also a function of the age of the suspension (or the shear history). The extent of the influence of the age of the suspension is seen in the propensity, or not, of the system to gel and hence in its plastic character; the ten minute gel strength measurements provide an indication of the magnitude of this effect. Thus, concentrated muds show a significant ageing effect but the dilute and thinned muds do not. The present data indicate that the application of the hydraulic stress will enhance the plastic nature; that is, thicken the mud, but only at elevated temperatures. We may speculate that the gel recovery process is not only a time-dependent phenomenon but that it is also a thermally activated process. Hence, the application of pressure has little influence on the plastic property at 20 °C, within the timescale of our experiment, but a significant enhancement may be achieved at temperatures above the critical gel restructuring temperature, T_R, described earlier. Above this restricting temperature, the application of the triaxial stress induces a relatively rapid enhancement of the plastic response. For the dilute and the thinned muds there is less potential for gel formation and hence less potential for a thermally activated restructuring process to enhance the yield stress. The recovery of the gel structure, as a result, is more rapid compared with that required for the concentrated muds.

In summary, it appears that the application of hydraulic stress will enhance the plastic character of the muds where the potential for such effects exist. The process is time-dependent and thermally activated. The viscous component of the response is generally less sensitive to the application of pressure for all the systems studied and does not appear to have a comparatively long characteristic time, thermally activated component of the type suggested for the plastic response. The structural, or restructuring, component of the viscous response has a relatively short relaxation time and is less sensitive to thermal activation.

It is now useful to examine the present data further, using what may be described as an effective volume model. Essentially, this is simply an application of the law of Corresponding States (Tabor 1991). Such treatments have been commonly applied to rationalize the rheology of particulate suspensions; this point is discussed later. It is apparent that the rheological response of these muds is a very strong function of the mean inter-particle separation distances (i.e. in our experiments this parameter may be varied by changing the bentonite concentration) at a fixed ionic strength. The time-dependent features discussed above are neglected for the moment. The conclusions to be proposed later, on this basis, will further support the proposed importance of these long time gel recovery processes and also their thermally activated nature. It is supposed that the hydrostatic compressibility and the thermal expansion of the solid particles themselves in muds, that is the clay and the barite particles, are essentially negligible; some experimental data were cited earlier to substantiate this assumption. The volume changes of the suspension under HPHT ambient conditions may be thus solely attributed to the behaviour of the liquid phase. For water, the measured isothermal compressibility at room temperature is $(4.1 \pm 0.15) \times 10^{-5}$ (1/bar) as obtained by the porosimeter method described in this study. The available literature also shows that this volume is approximately constant up to a temperature of 170 °C (Hoberock *et al.* 1982). Therefore, the 'effective' increase of the solid content, $\Delta\Phi_w$, due to the volume change of the liquid phase under pressure, P, under isothermal conditions, may be calculated using the following expression:

$$\Delta\Phi_w = \Phi_w C_{fm} P/(1 - C_{fm} P), \tag{12}$$

where C_{fm} is the compressibility of the mud, and Φ_w is the mass fraction of the clay particles. Thus, $\Delta\Phi_w$ corresponds to the increase to the mass fraction required to bring about the same response under ambient conditions.

There are a number of important precedents available in the literature which may be used to describe the influence of the volume fraction upon the rheology of particulate suspensions. These relations have been previously used to rationalize the response of the plastic viscosity property. The most notable, which are variants upon the Einstein equation, are due to Krieger (1972), Guth & Simha (1936), Gold (1937) and Simha (1952). All provide quite accurate means of fitting the available

Table 8. *The normalized plastic viscosities* $[\eta_{\text{pl}}]$ *at room temperature; experiments and the predictions from the model* (16)

(12% mud contains 0.5% $CaCl_2$; ratio of calculated model value to measurement value.)

mud (mass %)	T/°C	P/bar	experiment	model	ratio
8	26	700	1.04	1.02	0.98
8	26	1000	1.06	1.03	0.97
8	26	1350	1.08	1.05	0.97
10	21	1000	1.05	1.04	0.99
10	21	1350	1.13	1.06	0.94
12	22	700	1.04	1.03	0.99
12	22	1350	1.07	1.07	1.00

experimental data. Regrettably it is not feasible here to use volume fractions as the clay swells an undetermined amount in water. Instead, a pair of empirical relations, which describe, with sufficient accuracy, the yield stress and the plastic viscosity as a function of the clay weight fraction content, for these bentonite suspensions at room temperature, have been adopted (Appendix):

$$\tau_{\text{y}} = 0.60 \exp(33.46\varPhi_{\text{w}}) \tag{13}$$

and

$$\eta_{\text{pl}} = 4.43 \exp(10.55\varPhi_{\text{w}}). \tag{14}$$

Combining equations (12)–(14) provides two empirical relations which describe the normalized yield stress, $[\tau_{\text{y}}]$, and the normalized plastic viscosity, $[\eta_{\text{pl}}]$, at room temperature, as a function of the clay content and the hydrostatic stress;

$$[\tau_{\text{y}}] = \frac{\tau_{\text{y}}(P)}{\tau_{\text{y}1}} = \frac{\tau_{\text{y}}(1+\Delta\varPhi_{\text{w}})}{\tau_{\text{y}}} = \exp\left(\frac{33.46\varPhi_{\text{w}}C_{\text{fm}}P}{1-C_{\text{fm}}P}\right) \tag{15}$$

and

$$[\eta_{\text{pl}}] = \frac{\eta_{\text{pl}}(P)}{\eta_{\text{pl},1}} = \frac{\eta_{\text{pl}}(1+\Delta\varPhi_{\text{w}})}{\eta_{\text{pl}}} = \exp\left(\frac{10.55\varPhi_{\text{w}}C_{\text{fm}}P}{1-C_{\text{fm}}P}\right). \tag{16}$$

It may be observed that the exponential scalar term for $[\tau_{\text{y}}]$ is 33.46 and for $[\eta_{\text{pl}}]$ the corresponding value is 10.55. This indicates that the measured yield stress is much more sensitive to the clay content, real and effective, than the plastic viscosity. A comparison of the predictions of these relations with the experimental results obtained for plastic viscosities of concentrated muds at high pressures at room temperature (table 8) shows that the prediction of the plastic viscosity response is in good agreement, within the experimental and the analytical error, with the experimental data. However, the yield stress–pressure data, at room temperature, indicate that the yield behaviour may not be accurately interpreted by simply using the volumetric change argument (see table 9). We note also that the results reported by Sinha (1970), using a falling object viscometer, produced a similar conclusion. The origin of this discrepancy is considered further below.

At higher temperatures, the measured plastic viscosity was generally reduced in absolute terms (see table 4). This trend seems to be consistent with the effective volumetric change argument if we invoke the effects of the thermal expansion of the liquid phase. However, the effect of temperature on the yield behaviour of the muds

Table 9. *The normalized yield stress*, $[\tau_y]$; *experiments and the predictions from the model* (17)
(12% contains 0.5% $CaCl_2$; A_T is the temperature-dependent coefficient for the yield stress; ratio of calculated model value to measurement value.)

mud (mass %)	T/°C	A_T	P/bar	experiment	model	ratio
7	20	1.00	1000	0.98	1.10	1.12
8	20	1.00	700	1.03	1.08	1.05
10	20	1.00	1350	1.08	1.19	1.10
7	70	1.79	700	1.95	1.91	0.98
7	70	1.79	1000	2.04	1.97	0.97
8	65	2.10	700	2.35	2.27	0.97
8	65	2.10	1000	2.65	2.35	0.89
8	65	2.10	1350	2.90	2.43	0.84
8	80	3.05	1350	3.60	3.52	0.98
10	40	1.38	1000	1.62	1.56	0.98
10	40	1.38	1350	1.84	1.64	0.89
12	70	1.15	700	1.47	1.28	0.87
12	70	1.15	1350	1.89	1.63	0.86
12	115	1.65	1350	2.28	2.01	0.88

cannot be simply interpreted using the effective volumetric change model; see tables 3 and 4. It is seen that normalized plastic viscosity (normalized with respect to ambient temperature and pressure) does not show a simple variation with changes introduced in the pressure at relatively high temperatures. Obviously, the viscosity of the water decreases with the increase in the temperature and the reduction of the pressure. However, these effects are not large compared with the changes in the yield and flow behaviour observed for the muds. For example, for a 7% mud at 50 °C the application of pressure produces a 10% increase in the normalized viscosity which is comparable to the effect seen at around 20 °C and 70 °C. However, the 8% and 10% muds at 40 °C show a similar decrease in the normalized viscosity. Further, for the electrolyte doped systems, only marked decreases in the normalized viscosities are observed (table 4). Thus, apart from the volumetric phenomena discussed above, thermally induced electrochemical variations, introduced by thermally promoted changes in the ionic strength, on the clay particle interactions may play an important role. We have not studied the variation of the ambient electrolyte concentration with temperature and pressure in detail. The limited data and its significance were mentioned earlier. It has been shown that the yield values of the clay muds, at higher temperatures, is strongly dependent on the clay content, the electrolyte concentration and the other chemicals added (Ren 1992). To produce a general relationship which describes the effects of both the pressure and the temperature on the yield behaviour of the clay suspensions, (15) may be modified by a temperature-dependent coefficient, A_T, which is a function of the temperature, the clay content, the electrolyte concentration and the other variables involved; e.g. pH. A generalized equation is given as

$$[\tau_y] = A_T \exp[S_y \Phi_w C_{fm} P/(1 - C_{fm} P)], \tag{17}$$

where A_T may be obtained from the yield stress measurements at elevated temperatures and at atmospheric pressure. Simply, $A_T = 2$ means that the yield stress of the mud increases by a factor of two as temperature is raised from room ambient to T. S_y is the exponential value of the yield stress–clay content relationship at the chosen temperature. Because the yield behaviour of the muds becomes more sensitive to the clay content at higher temperatures, the value of S_y should be higher than, or at least equal to, 33.46 (see equation 13) for the room temperature case. Here, we have taken $S_y = 33.46$ as a conservative estimate. These results indicate that the measured yield stress seems to be reasonably predicted by (17). For example, the calculated normalized yield stress from the measurement on an 8% mud, at a pressure of 1350 bar and a temperature of 80 °C, is 3.60; the predicted value from the above model is 3.52 ($A_T = 3.05$ from table 9). In other conditions, a 10% mud at $P = 1350$ bar, $T = 40$ °C and $A_T = 1.38$, the measured value is 1.84, and the corresponding predicted value is 1.63. The comparisons of the experimental results with the predicted values for other samples are in table 9.

The results of the comparison of the model with the experimental results are not unexpected. The model over-predicts the yield stress at room ambient; the structure has not fully developed its long range order to enhance the gel strength. At higher temperatures, the model under-predicts the influence of the density change and presumably the thermal activation has facilitated the development of the gel within the time scale of experiment. The experimental result suggests that the pressure effect on the rheology of the muds may be attributed mainly to a physically induced compression of liquid phases of the suspension. However, the effect of temperature, which is described simply by the temperature coefficient, A_T, in (17), is a complicated function of the composition of the system, and the parameter must be determined, by experiment, for each mud sample. Some of the effects noted appear to be associated with electrochemical factors, e.g. the varying levels of ionic strength in the aqueous medium. This aspect is discussed further at the conclusion of the paper.

5. Conclusions

The rheological properties, particularly the yield behaviour, of concentrated bentonite suspensions are sensitive to the ambient temperature and pressure. A substantial enhancement of the gel structure of the muds at higher temperatures may be attributed to the thermally induced activity of the bentonite particles, enabling the gel structure of the clay to be formed within the timescale of the experiment. This results in an increase of the yield stress. The extent of the temperature effect is strongly dependent on the composition of the muds. The addition of additives, such as simple electrolytes, can effectively inhibit the swelling or compress the electrical double layers associated with the clay particles so that a much weaker gel is formed. As a result, the yield behaviour of these thinned muds becomes less temperature sensitive. This is, in fact, one of the practical methods available for the stabilization of the field muds for high temperature wells.

It has been found that pressure has a considerable effect on the yield stress of concentrated bentonite muds at low ionic strengths; these effects are also temperature and clay content dependent. At higher temperatures, the yield stress of the concentrated muds increases gradually with the increasing of the pressure. However, at room temperature, a pressure up to 1400 bars has a minimal effect on the yield stress of the muds with clay content up to 9% (mass) within the timescale of the present experiments.

On the other hand, the effects of temperature and pressure have been found to be not significant in terms of the variation of plastic viscosity. The data suggest that at high temperatures and pressures the plastic viscosity, or high shear limiting viscosity, may decrease, particularly in the presence of electrolytes. The rheological behaviour of barite-loaded muds at high pressures and high temperatures is mainly dependent on the properties of the base-muds. The proposed expressions for calculating the densities and sonic velocities of muds are useful for the assessment of the properties of drilling fluids at downhole conditions.

In summary, the data confirm that the rheology of the various muds may be described well using the Bingham approximation under certain conditions. The changes induced in both the viscous and plastic components of the response are described well by the effective volume argument, which supposes that the alteration of the ambients changes the inter-particle distances and the rheology of continuous phase in an additive way. It appears that the plastic component, τ_y, which reflects the gel strength, is a time-dependent property which may require thermal activation to produce rapid gelation. It will be realized that this proposed time-dependent restructuring is a phenomenon which will be apparent upon the application of a *quasi*-instantaneous pneumatic stress under isothermal conditions. Presumably, both the density and the rheology will change in a time-dependent way as the system restructures. Such effects are rather well established in polymeric systems and in complex liquids where the process is termed viscoelastic retardation in compression (Duckett & Joseph 1976; Harrison & Trachman 1972; Briscoe & Smith 1982). In the case of polymers, long range molecular rearrangements are required in order to develop the equilibrium structure associated with the new state. The volume changes, and so does the rheology, in a progressive way. We may suppose that similar, long range, restructuring processes occur with clay gels. A critical restructuring temperature is proposed, along the lines suggested by previous researchers, which marks the temperature where the timescale for restructuring becomes apparently instantaneous. The much higher gel disruption temperature, T_D, has not been detected in this study. We thus conclude that, although the Bingham model is effective, its general use requires that the parameter, τ_y, be given time and temperature dependent descriptors.

Finally, certain trends in the variations of the plastic viscosity are not interpretable using the induced volumetric change model and we have proposed that thermally promoted electrolyte dissolution, from clay and barite particles, may be responsible for the reductions noted in the normalized plastic viscosity at elevated temperatures and pressures, in certain instances. An increase in ionic strength effectively reduces the sphere of influence of the particles and hence their effective volume fraction.

In conclusion, the data support the notion that inter-particle interactions are largely responsible for the rheological characteristics of these systems. The sphere of influence of each particle, and hence its degree of interaction with its neighbours, may be changed by dilution and by volume changes in the continuous phase induced by hydrostatic compression or thermal expansion of the liquid phase, or by modification of electrochemical interactions. In this way the behaviour of the systems may be predicted using the law of Corresponding States in a reasonably accurate way. In some circumstances, particularly where interactions are strong and of a long range, there may be time-dependent effects associated with the progressive evolution in the relative spatial disposition of particles. Where the particle–particle interactions are strong, the relative influence of the changes in the rheology of the continuous phase *per se* are small but as the particle interactions are weakened, the variations in the rheology of the superincumbent fluid become noticeable.

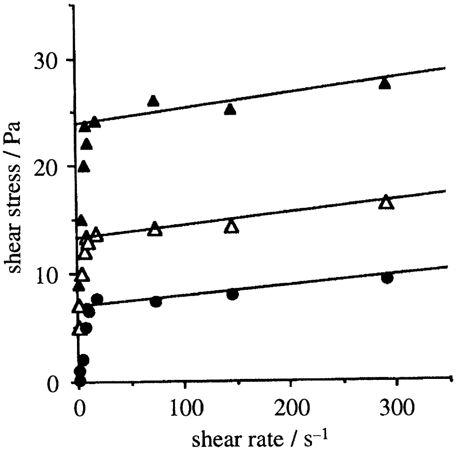

Figure 13. Shear stress against shear rate measured for various bentonite suspensions. Clay content: ● 7%; △ 9%; ▲ 11%.

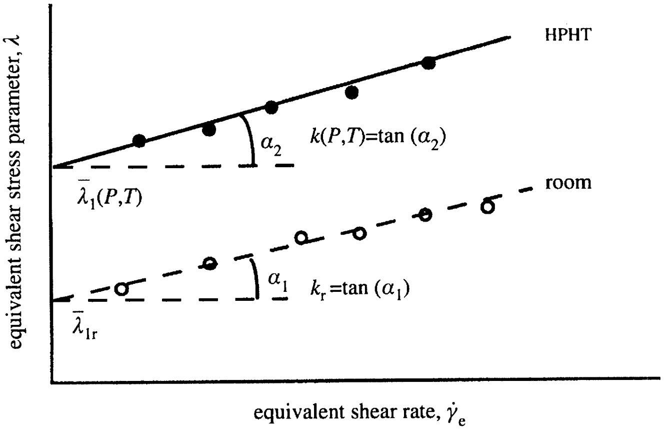

Figure 14. The rheograms plotted for the data of the HPHT rolling-ball rheometer at room condition and under HPHT conditions showing the determination of the extrapolated Bingham parameters.

We thank Dr M. Abudaka, R. King and P. Amrit for help in construction of the high pressure rolling-ball rheometer. Financial support from the British Council to S.R.R. is also appreciated.

Appendix A. Determination of the extrapolated Bingham parameters

The rheological properties of concentrated muds as determined from a conventional concentric cylinder Bohlin rheometer are given in figure 13. The data may be fitted well using the Bingham equation (1) and show the characteristic increase in the Bingham yield value, τ_B, with increasing clay concentration. We may also define an extrapolated yield value, τ_y, which corresponds to the extrapolation of the linear portion of the graph to zero shear rate. It is the extrapolated yield stress which we may measure using the rolling-ball rheometer. For the muds, τ_B and τ_y have similar values enabling (1) to be used in the modelling procedures described in the text of this paper.

Figure 14 shows an example of how the normalized (extrapolated) yield stress and plastic viscosity are determined from the rheogram of the rolling-ball rheometer. The intercept of the linearly fitted $\bar{\lambda}$–$\dot{\gamma}_e$ curve, $\bar{\lambda}_1$, relates to the yield stress by a

Figure 15

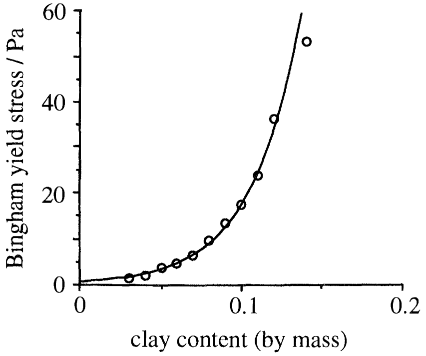

Figure 16

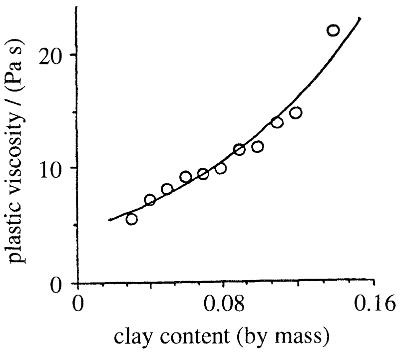

Figure 15. Computed Bingham yield stress as a function of clay weight fraction at 20 °C and 1 atm (= 101325 Pa). $\tau_y = 0.60 \exp(33.46\, C_\Phi)$.

Figure 16. Computed Bingham plastic viscosity as a function of weight fraction. $P_v = 4.43 \exp 10.55\, C_\Phi$.

factor of F; $\tau_y \propto F\bar{\lambda}_1$ and the slope of the curve, k, relates to the plastic viscosity as $\eta_{pl} \propto F'k$ (Briscoe *et al.* 1992*b*). According to equations 6 and 7, the normalized parameters may be calculated simply as

$$[\tau_y] = \tau_y(P,T)/\tau_{y,1} = \bar{\lambda}_1(P,T)/\bar{\lambda}_{1r} \tag{A 1}$$

and

$$[\eta_{pl}] = \eta_{pl}(P,T)/\eta_{pl,1} = k(P,T)/k_r, \tag{A 2}$$

where $\bar{\lambda}_{1r}$ and k_r refer to the parameters obtained for room conditions, and $\bar{\lambda}(P,T)$ and $k(P,T)$ refer to the high pressure and temperature conditions as shown in figure 14.

Figures 15 and 16 show data obtained by these means for the Bingham yield stress and the plastic viscosity respectively as a function of clay content (mass fraction) at ambient conditions. The data have been fitted to the expressions shown in the main text as equations (13) and (14) for the yield and viscous parameters respectively.

References

Alderman, H. J., Gavignet, A., Guillot, D. & Maitland, G. C. 1988 High temperature and high pressure rheology of water-based muds. SPE paper 18035, SPE Meeting, Houston. Dallas: SPE.

Annis, M. R. 1967 High temperature flow properties of water-base drilling fluids. *J. Petrol. Technol.* **19**, 1074–1080.

Beris, A. N., Tsampoulos, J. A., Armstrong, R. C. & Brown, R. A. 1985 Creeping motion of sphere through a Bingham plastic. *J. Fluid Mech.* **158**, 219–244.

Bingham, E. 1922 *Fluidity and plasticity*. New York: McGraw-Hill.

Briscoe, B. J., Luckham, P. F. & Ren, S. R. 1992*a* The falling of spheres through Bingham fluids. *Colloids Surfaces* **65**, 69–75.

Briscoe, B. J., Luckham, P. F. & Ren, S. R. 1992*b* An assessment of a novel rolling-ball rheometer for studying non-newtonian fluids. *Colloids Surfaces* **62**, 153–162.

Briscoe, B. J., Luckham, P. F. & Ren, S. R. 1992*c* The rheological properties of barite-loaded drilling fluids. *Trans. Instn. chem. Engrs* **70**, 55–62.

Briscoe, B. J. & Smith, A. C. 1982 Time dependent effects in the shear of thin polymeric films. *J. Phys.* D **15**, 579–594.

Briscoe, B. J. & Zakaria, S. 1992 Sorption and dilation of silicone elastomer composites at high pressure – the role of interfacial quality. *J. Polymer Sci.* B **30**. 956–969.

Duckett, R. A. & Joseph, S. H. 1976 Time dependent effects of pressure on the shear modulus of polypropylene. *Polymer* **17**, 329–334.

Gold, O. 1937 Ph.D Thesis, Vienna University.

Gray, G. R. & Darley, H. C. H. 1980 *Composition and properties of oil well drilling fluids*. 4th edn, pp. 231–250. Gulf.

Guth, E. & Simha, R. 1936 *Kolloidzeitschrift* **74**, 266.

Harrison, G. & Trachman, E. G. 1972 The role of compressional viscoelasticity in the lubrication of rolling contacts. *Trans. Am. Soc. mech. Engrs* **94**, 306–312.

Hiller, K. H. 1963 Rheological measurements on clay suspensions and drilling fluids at high pressures and high temperatures. *J. Petrol. Technol.* **15**, 779–790.

Hoberock, L. L., Thomas, D. C. & Nikens, H. V. 1982 Here's how compressibility and temperature affect bottom-hole mud pressure. *Oil Gas J.* **80**, 159–164.

Krieger, I. M. 1972 *Adv. Colloid Interface Sci.* **3**, 111–136.

Kutasov, I. M. 1988 Empirical correlation determining downhole mud density. *Oil Gas J.* **86**, 61–63.

McMordie, W. C., Bland, R. G. & Hauser, J. M. 1982 Effect of temperature and pressure on density of drilling fluids. SPE paper 11114, SPE Meeting, New Orleans. SPE.

Perry, R. H. & Green, D. 1985 *Perry's chemical engineers' handbook*. 6th edn. New York: McGraw-Hill.

Reid, R. C., Pransnitz, J. M. & Shearwood, T. K. 1977 The properties of gases and liquids. 3rd edn. New York: McGraw-Hill.

Ren, S. R. 1992 Rheology of clay suspensions at high pressure. Ph.D. thesis, Department of Chemical Engineering, Imperial College, U.K.

Simha, R. 1952 *J. appl. Phys.* **23**, 1020–1024.

Sinha, B. K. 1970 A new technique to determine the equivalent viscosity of drilling fluids under high pressure and temperature. *SPE J.* **10**, 33–40.

Smalley, M. V., Thomas, R. K., Braganza, L. F. & Matsuo, T. 1989 Effect of hydrostatic pressure on the swelling of *n*-butylammonium vermiculite. *Clays clay minerals* **37**, 474–478.

Tabor, D. 1991 *Gases, liquids and solids*, 3rd edn. Cambridge University Press.

Wilson, W. D. 1959 Speed of sound in distilled water as a function of temperature and pressure. *J. acoust Soc. Am.* **31**, 1067–1072.

Wilson, W. D. 1960 Equation of the speed of sound in sea water. *J. acoust. Soc. Am.* **32**, 1537–1540.

Wilson, W. D. 1962 Extrapolation of the speed of sound in sea water. *J. acoust. Soc. Am.* **34**, 866–868.

Received 6 August 1992; accepted 28 May 1993